Downregulation of inhibitor of apoptosis protein induces apoptosis and suppresses stemness maintenance in testicular teratoma

GANG LI*, MAN LIAO*, SHUANG LI, JIA YOU, JUN WANG, WEI LEI, CHUNLEI YANG, HAOLUN XU, HE XIAO and HAITAO CHEN

Department of Urology, Wuhan Children's Hospital, Wuhan, Hubei 430016, P.R. China

Received September 17, 2020; Accepted June 23, 2021

DOI: 10.3892/etm.2021.10835

Abstract. Inhibitors of apoptosis (IAPs) are a family of cell death inhibitors found in viruses and metazoans that physically interact with a variety of pro-apoptotic proteins and inhibit apoptosis induced by diverse stimuli. Melanoma IAP (ML-IAP) is a potent anti-apoptotic protein that is strongly upregulated in melanoma and confers protection against a variety of pro-apoptotic stimuli. In the present study, it was revealed that ML-IAP was expressed at high levels in testicular teratoma. Deletion and mutational analysis demonstrated that ML-IAP silencing significantly decreased P19 cell proliferation while inducing cell cycle arrest and apoptosis. ML-IAP knockdown significantly induced caspase-3/8/9-mediated apoptosis in P19 cells. In addition, metabolism and stemness maintenance in P19 cells were suppressed by ML-IAP knockdown. These results indicated that ML-IAP silencing is a powerful inducer of apoptosis mediated by cell death receptors and may function as a direct activator of downstream effector caspases.

Introduction

Germ cell tumors account for ~60-77% of testicular tumors (1) and are the main cause of cancer in men between 15-35 years of age (2). A previous study has revealed that children with solid tumors, primary prepubertal testis tumors, para-testicular tumors and testicular teratomas account for 50.8% (3). Consequently, it is particularly urgent to investigate the occurrence and developmental mechanism of testicular teratoma and to identify its therapeutic targets.

Inhibitor of apoptosis proteins (IAPs) are a family of proteins that play important roles in regulating programmed cell death or apoptosis (4). There are 8 mammalian IAPs: XIAP, c-IAP1, c-IAP2, hILP-2, ML-IAP, NAIP, survivin and Apollon (5). Kocab and Duckett (6) revealed that IAPs were highly expressed in 32 types of malignant solid tumors (6). IAPs play critical roles in mediating the survival and death of various cells by regulating key factors such as caspase activation and nuclear factor-κB signaling (7,8). Rada *et al* reported that XIAP, BIRC2, and BIRC3 promoted the anti-apoptotic ability of ovarian cancer cells by regulating nuclear factor-κB signaling (9). In a non-small cell lung cancer cell line, IAP inhibitors reduced the protein expression of c-IAP2 and XIAP and enhanced cisplatin-induced apoptosis by activating caspase pathways (10). However, the expression of IAPs in testicular teratoma and their effect on testicular teratoma cells have rarely been reported.

Cancer stem cells (CSCs) are small subpopulations present in tumor cells that are considered as the source of tumorigenicity (11). The presence of CSCs in solid tumor tissues can counteract current common therapeutic drugs (12). In CSCs, aberrantly increased cell metabolism can promote tumorigenesis and metastasis (12). The effect of drugs can be significantly improved by inhibiting the Warburg effect in tumor cells (13,14). Studies have confirmed that the Warburg effect is related to changes in the tumor microenvironment, mitochondrial function, and aberrant expression of glucose metabolism enzymes, which help tumor cells escape apoptosis and promote tumor metastasis (15,16). Ji *et al* (17) revealed that XIAP plays an important role in maintaining CSCs in nasopharyngeal carcinoma. Ausserlechner and Hagenbuchner (18) reported that survivin inhibitors reduced the activation of the Warburg effect and promoted the drug sensitivity of neuroblastoma cells. However, the effects of IAPs on the Warburg effect and stemness maintenance in testicular teratoma have not been reported.

In the present study, the expression of ML-IAP in testicular teratoma was evaluated and it was investigated whether ML-IAP inhibition could regulate glycolysis, stemness maintenance, and apoptosis in testicular teratoma cells.

Materials and methods

Tissue samples. Testicular teratoma tissues and para-carcinoma tissues were obtained from 20 patients (age range, 4 months to 11 years old) from August 2018 to 2019, who were

Correspondence to: Dr Man Liao, Department of Urology, Wuhan Children's Hospital, 100 Xianggang Road, Wuhan, Hubei 430016, P.R. China
E-mail: 1214497823@qq.com

*Contributed equally

Key words: testicular teratoma, inhibitor of apoptosis proteins, apoptosis, caspase pathway, Warburg effect, stemness maintenance

treated at Wuhan Children's Hospital (Wuhan, China). All operations were approved by the Ethics Review Committee of Wuhan Children's Hospital, and the guardians of all patients provided written informed consent to participate in the present study and to provide samples for subsequent experiments.

Cell culture. P19 mouse testicular teratoma cells (the most common cell line, which is widely used in basic experimental studies of human testicular teratoma) were purchased from the Type Culture Collection of the Chinese Academy of Sciences and cultured in α-modified Eagle's medium (cat. no. SH30265.01; Hyclone; Cytiva) supplemented with 10% fetal bovine serum (FBS; cat. no. 1027-106; Gibco; Thermo Fisher Scientific, Inc.) at 37˚C in an atmosphere containing 5% CO_2.

Cell transfection. ML-IAP-NM_001163247 vectors (ML-IAP overexpression), empty vectors (negative control or NC), short interfering (sh)ML-IAP vectors (ML-IAP interference), and shNC were constructed by Wuhan Myhalic Biotechnology Co., Ltd. The vectors (4 μg) were transfected into P19 cells ($5x10^5$) using Lipofectamine™ 2000 (Invitrogen; Thermo Fisher Scientific, Inc.) according to the manufacturer's instructions at 37˚C for 48 h before subsequent experiments. Untransfected P19 cells were treated as control. Cells were maintained in Dulbecco's modified Eagle's medium (cat. no. SH30265.01; Hyclone; Cytiva) with 10% FBS and cultured at 37˚C in humidified air with 5% CO_2.

3-(4,5-Dimethylthiazol-2-yl)-2,5-diphenyltetrazolium bromide (MTT) assay. Cell proliferation was determined by MTT assay (Sigma-Aldrich; Merck KGaA). A total of $5x10^3$ cells were seeded in 96-well plates and 20 μl of MTT (5 mg/ml) was added to each well and incubated for 4 to 6 h at 37˚C. At the end of the incubation period, the medium was removed and 150 μl of dimethyl sulfoxide was added to each well. After shaking at low speed for 10 min, the absorbance of converted dye was measured at a wavelength of 490 nm.

Biochemical analysis. Levels of caspase-3 was evaluated using caspase-3 activity assay kit (cat. no. c1116; Beyotime Institute of Biotechnology) according to the manufacturer's instructions.

RNA extraction and quantitative reverse transcription polymerase chain reaction (RT-qPCR). Total RNA (from P19 cells) was extracted from samples using TRIzol reagent (Ambion; Thermo Fisher Scientific, Inc.) following the manufacturer's instructions. RNA (500 ng) was transcribed to cDNA in a final volume of 10 μl using the PrimeScript® RT reagent kit with gDNA Eraser (Takara Bio, Inc.) according to the manufacturer's protocol. Quantitative PCR was performed using a SYBR Green PCR Kit (Kapa Biosystems; Roche Diagnostics) according to the manufacturer's instructions. The primer sequences are listed in Table I. The RT-qPCR results were normalized to the expression of GAPDH and analyzed as the fold change [$2^{-\Delta\Delta Cq}$ (19)]. The quantitative PCR reaction for each sample was performed in triplicate.

Western blot analysis. P19 cell were washed in phosphate-buffered saline (PBS) and lysed using radioimmunoprecipitation assay buffer (Invitrogen; Thermo Fisher Scientific, Inc.). A bicinchoninic acid (BCA) assay was performed to determine the protein concentration and equivalent amounts of proteins (20 μg/lane) from each sample were electrophoresed by 12% sodium dodecyl sulfate-polyacrylamide gel electrophoresis. The proteins were transferred to a polyvinylidene fluoride membrane, blocked in 4% skim milk for 2 h at room temperature, and incubated at 37˚C for 1 h with specific primary antibodies against the following proteins: ML-IAP (1:1,000; cat. no. PAB34211), Bax (1:1,000; cat. no. PAB30861), Bcl-2 (1:1,000; cat. no. PAB33482), caspase-3 (1:1,000; cat. no. PAB33236), caspase-8 (1:1,000; cat. no. PAB30048), caspase-9 (1:1,000; cat. no. PAB40626), glucose transporter (GLUT)1 (1:1,000; cat. no. PAB40969), lactate dehydrogenase-A (LDHA; 1:1,000; cat. no. PAB30703) and hexokinase (HK)1 (1:1,000; cat. no. PAB30519; all from Bioswamp Wuhan Beinle Biotechnology Co., Ltd.). GAPDH (1:1,000; cat. no. PAB36269; Bioswamp Wuhan Beinle Biotechnology Co., Ltd.) was used as a loading control. Horseradish peroxidase-linked goat anti-rabbit IgG (1:20,000; cat. no. SAB43714; Bioswamp Wuhan Beinle Biotechnology Co., Ltd.) was used as the secondary antibody at 37˚C for 1 h. Immunoreactivity was visualized by colorimetric reaction using an enhanced chemiluminescence substrate buffer (EMD Millipore). The membranes were scanned with Gel Doz EZ imager (Bio-Rad Laboratories, Inc.) and images were processed using ImageJ software version 1.8.0 (National Institutes of Health).

Cell cycle assay. The cell cycle of P19 cells ($1x10^7$) was assessed by flow cytometry. The cells were washed three times with ice-cold PBS and fixed with 70% (v/v) ethanol for 1 h at -20˚C. After another PBS wash, a staining solution containing 10 mM Tris (pH 7.0), 0.1% NP-40, 1 mM NaCl, 0.7 μg/ml ribonuclease A and 5 μg/ml propidium iodide (PI) was added to the cells. After 30 min of incubation in the dark at 37˚C, cellular DNA content was examined by PI-staining flow cytometry (FC500 MCL; Beckman Coulter, Inc.), Data were analyzed with the CytExpert software version 2.0 (Beckman Coulter, Inc.).

Immunohistochemical staining. Paraffin-embedded samples of testicular teratoma tissues and para-carcinoma tissues (5-μm) were fixed at 10% formalin for 48 h at 37˚C, then stained for ML-IAP. The sections were deparaffinized in xylene and rehydrated in a graded series of ethanol, followed by heat-induced epitope retrieval in citrate buffer (pH 6.0). Antigen retrieval was performed in 10 mmol/l citrate buffer (pH 6.0) in a microwave oven for 15 min. Endogenous peroxidase activity was blocked by 3% hydrogen peroxide for 10 min at room temperature. ML-IAP antibody (1:50) was applied overnight at 4˚C, and after three washes in PBS, the sections were immunostained with ML-IAP MaxVision ™HRP-Polymer anti-Mouse/Rabbit IHC Kit (1:50, cat. no. PAB34211; Bioswamp Wuhan Beinle Biotechnology Co., Ltd.) for 1 h at 37˚C. After three rinses in PBS, the sections were developed with 3,3'-diaminobenzidine and counterstained with hematoxylin for 3 min at 25˚C and the sections were observed using an optical microscope (MD1000; Leica Microsystems GmbH).

Table I. Primers used in the reverse transcription-quantitative PCR.

Gene name	Forward primer (5'→3')	Reverse primer (5'→3')
XIAP	GCAGACATCAATAAGGA	TGAAACAGGACTACCAC
c-IAP1	AAAGAGAAGAGGAGAAGGA	CAGGATAGGAAGCACACA
c-IAP2	TTCCACACACTCATTACTTC	ATTTTCCACCACAGGC
hILP-2	ACTGTGGAGGAGGGCTA	GTGATGGTGTTTTCTTGGTA
ML-IAP	ATGGGACCTAAAGACAGT	CAGACGCAACTCCTCA
NAIP	GACATCTCCAGGCATT	CCTTGGTAGTCGTAACAC
Survivin	ACCACCGCATCTCTAC	GGCTCTTTCTCTGTCCA
Apollon	CTATTTCTGCCGTGAT	TGGTTGGCTAAGACTAA
SOX2	AGCGGCGTAAGATGGC	TCGGTCTCGGACAAAAGTT
Bmi1	AATGTGTGTCCTGTGTGG	GGAGTGGTCTGGTTTTGT
OCT4	TTCAGCCAGACCACCATC	CGGGCACTTCAGAAACAT
Nanog	TACCAGTCCCAAACAAAAGC	TGAGAGAACACAGTCCGCAT
GAPDH	CCACTCCTCCACCTTTG	CACCACCCTGTTGCTGT-3'

ML-IAP, melanoma IAP; OCT4, octamer-binding transcription factor 4; SOX2, sex determining region Y-box 2.

Statistical analysis. The statistical differences in the experimental data were evaluated by one-way analysis of variance (ANOVA) followed by Dunnett's post hoc test using the SPSS 19.0 software package (IBM Corp.). $P<0.01$ was considered to indicate a statistically significant difference. All results were expressed as the mean ± standard deviation (SD).

Results

ML-IAP is upregulated in testicular teratoma. The mRNA expression levels of IAP family members (XIAP, c-IAP1, c-IAP2, hILP-2, ML-IAP, NAIP, survivin and Apollon) in testicular teratoma and para-carcinoma were detected by RT-qPCR (Fig. 1A). The mRNA expression levels of ML-IAP and survivin were significantly higher in testicular teratoma compared with those in para-carcinoma tissues, as was the protein expression of ML-IAP (Fig. 1B). Immunohistochemistry also revealed that ML-IAP was expressed to a greater extent in testicular teratoma (Fig. 1C). These results indicated that ML-IAP may play an important role in the development of testicular teratoma.

Downregulation of ML-IAP inhibits P19 cell proliferation. The effect of ML-IAP in testicular germ cell tumors was investigated using ML-IAP overexpression or interference vectors. As revealed in Fig. 2A and B, ML-IAP interference and overexpression vectors significantly decreased and increased the expression of ML-IAP in P19 cells, respectively. In addition, ML-IAP interference significantly suppressed the proliferation of P19 cells (Fig. 2C).

Downregulation of ML-IAP induces cell cycle arrest in P19 cells. The observation that ML-IAP interference inhibited cell proliferation led us to investigate the effect of ML-IAP on cell cycle progression, which was assessed by PI-staining flow cytometry (Fig. 3). G_1 phase was reduced while the S phase and G_2 phase was slightly increased in shML-IAP transfected-cells compared with the shNC group, while ML-IAP repaired the arrest and promoted cell cycle progression. These results indicated that ML-IAP knockdown induced P19 cell cycle arrest in the G_2 phase.

Downregulation of ML-IAP induces P19 cell apoptosis. The expression of proteins associated with apoptosis was detected in P19 cells by western blot analysis. (Fig. 4A). ML-IAP interference induced a significant increase in the expression of the pro-apoptosis proteins Bax, caspase-3, caspase-8, and caspase-9 in P19 cells, while inhibiting the expression of the anti-apoptosis protein Bcl-2. Caspase-3 activity was further detected by biochemical tests, and the results also supported the foregoing conclusion (Fig. 4B). The results indicated that ML-IAP silencing activated caspase-mediated apoptosis.

Downregulation of ML-IAP inhibits metabolism and stemness maintenance in P19 cells. The expression of cell metabolism-related proteins was detected by western blot analysis. The shML-IAP-transfected cells revealed lower levels of GLUT1, HK1, and LDHA compared with non-transfected cells (Con), while the protein levels of GLUT1, HK1, and LDHA in ML-IAP-overexpressing cells were higher than those in non-transfected cells (Fig. 5A). Concurrently, inhibition of ML-IAP significantly downregulated the stemness factors Bmi1, Nanog, octamer-binding transcription factor 4 (OCT4) and sex determining region Y-box 2 (SOX2) at the mRNA level in P19 cells (Fig. 5B).

Discussion

Testicular germ cell tumors are the most common malignancies among young men (20). The present study revealed that the expression of ML-IAP was increased in patients with testicular germ cell tumors, and ML-IAP silencing reduced the proliferation, induced the apoptosis, and inhibited the stemness maintenance of P19 testicular teratoma cells by regulating caspase-mediated pathways and the Warburg effect.

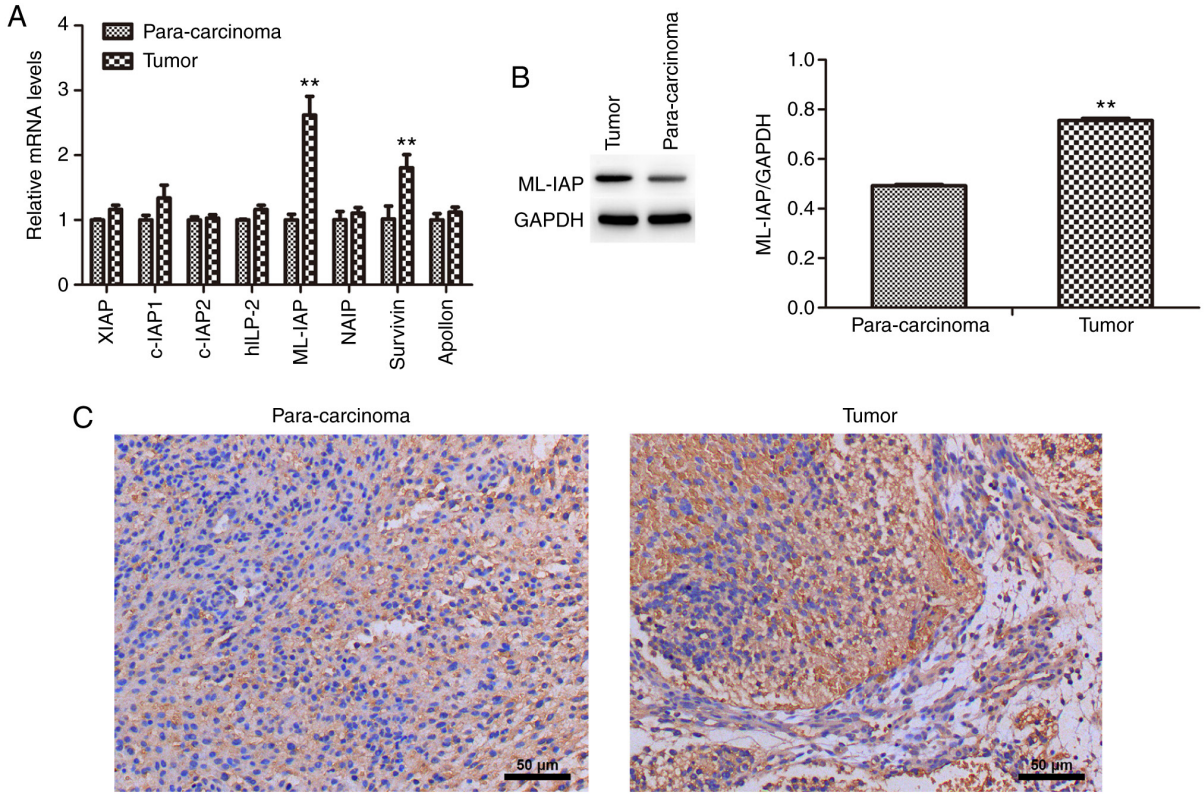

Figure 1. ML-IAP is expressed at high levels in testicular teratoma. (A) The mRNA expression levels of IAP family members in testicular teratoma and para-carcinoma tissue were detected by reverse transcription-quantitative PCR. (B) The protein expression of ML-IAP in testicular teratoma and para-carcinoma tissue was detected by western blot analysis. (C) The expression of ML-IAP in testicular teratoma and para-carcinoma tissue was evaluated by immunohistochemistry. Data are presented as the mean ± SD (n=3). **P<0.01 vs. para-carcinoma. ML-IAP, melanoma IAP; IAP, inhibitor of apoptosis.

Viability assays have revealed that ML-IAP is a powerful inhibitor of apoptosis induced by death receptors and chemotherapeutic agents (21). ML-IAP is upregulated in most melanoma cell lines examined and has been revealed to contribute to the chemoresistance of this disease (22). Several studies have revealed that ML-IAP functions as a direct and specific inhibitor of caspases 3 and 9 (23,24). In the present study, it was identified that ML-IAP was expressed at high levels in testicular teratoma. The expression of ML-IAP in P19 cells was then regulated by transfecting them with overexpression or interference plasmids, and it was demonstrated that ML-IAP interference significantly inhibited P19 cell proliferation while inducing cell cycle arrest. Furthermore, downregulation of ML-IAP induced apoptosis by activating the caspase-3/8/9 pathway in P19 cells. Cancer cells are often characterized by increased resistance to apoptosis, which enables their survival under aberrant growth stimulation and mediates their augmented resistance to various forms of cellular stress, such as hypoxia, DNA damage and nutrient deprivation (25). Thus, the finding that ML-IAP downregulation contributed to P19 cell apoptosis may provide a rational basis for the development of novel therapeutic strategies that specifically regulate the activity of apoptotic pathways in tumor cells.

Tumor cells produce a large amount of lactic acid through aerobic glycolysis while reducing mitochondrial oxidative phosphorylation through the phenomenon known as the Warburg effect (26). The metabolic reactions of glycolysis are catalyzed by numerous enzymes, among which GLUTs,

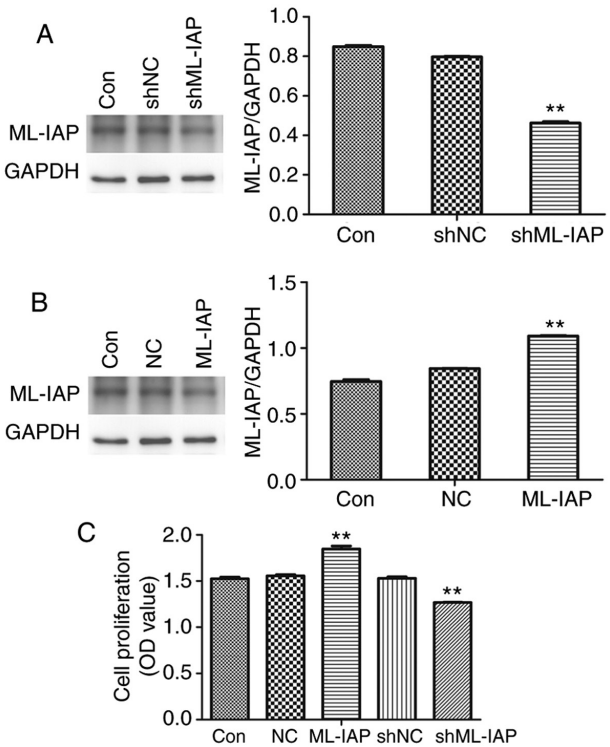

Figure 2. Downregulation of ML-IAP inhibits P19 cell proliferation. P19 cells were transfected with (A) interference or (B) overexpression vectors of ML-IAP and the protein expression of ML-IAP was detected by western blot analysis. (C) P19 cell proliferation was detected by MTT assay. Data are presented as the mean ± SD (n=3). **P<0.01 vs. Con. ML-IAP, melanoma IAP; sh, short hairpin; NC, negative control.

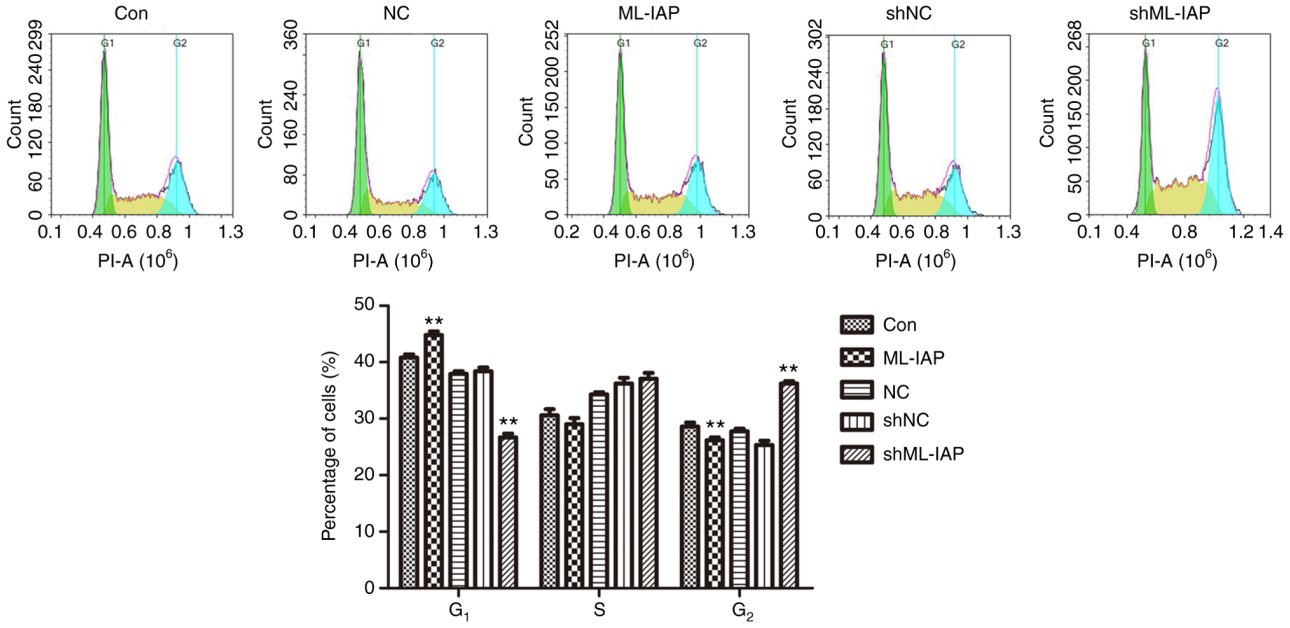

Figure 3. Downregulation of ML-IAP induces cell cycle arrest in P19 cells. The cell cycle distribution of P19 cells was assessed by flow cytometric analysis. Representative histograms and the percentage of cells in each phase of the cell cycle are plotted as the mean ± SD (n=3). **P<0.01 vs. Con. ML-IAP, melanoma IAP; sh, short hairpin; NC, negative control.

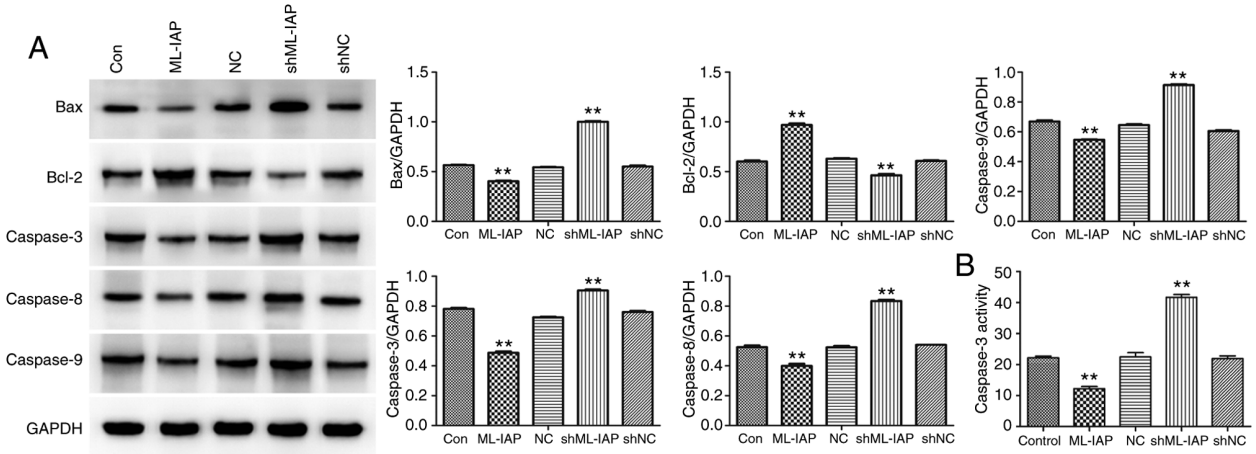

Figure 4. Downregulation of ML-IAP induces the activation of caspase-mediated apoptosis in P19 cells. (A) The levels of apoptosis-associated proteins Bax, Bcl-2, caspase-3, caspase-8 and caspase-9 in P19 cells were detected by western blotting. (B) Caspase-3 activity was evaluated by biochemical detection. Data are presented as the mean ± SD (n=3). **P<0.01 vs. Con. ML-IAP, melanoma IAP; sh, short hairpin; NC, negative control.

HK1, LDHA and pyruvate kinase M2 (PKM2) are implicated in cancer (27). GLUT1 reportedly exhibited high expression profiles in numerous tumors, and increased GLUT1 is involved in the activation of mammalian target of rapamycin, leading to an increase in glycolysis (28). In the present study, the protein expression levels of GLUT1, HK1, and LDHA in P19 cells were significantly decreased by ML-IAP knockdown, indicating that glycolysis was inhibited by ML-IAP silencing in P19 cells.

Cancer metabolism may be associated with the persistence of CSC metabolism, which forms the basis of the Warburg effect in cancer. Owing to their special biological properties, CSCs are considered to play key roles in tumor initiation, resistance to chemotherapy and radiotherapy, and disease recurrence (29). Notably, certain regulatory pathways known to govern cell metabolism and energy sensing are involved in maintaining the self-renewal property of CSCs. CSCs possess increased self-renewal and differentiation abilities and express high levels of stemness genes including Nanog, SOX2, OCT4, and Bmi1 (30,31). Our results indicated that downregulation of ML-IAP expression in P19 cells inhibited the expression of stemness factors (Bmi1, Nanog, OCT4, and SOX2). It was hypothesized that the inhibition of stemness maintenance in P19 cells by ML-IAP downregulation may be associated with the suppression of the Warburg effect.

In the present study, the MTT experiment was used to detect the cell proliferation. The CCK-8 experiment and cell counting results may provide more accurate results, but it is considered that the results from the MTT experiment are sufficient. Additionally, P19 cells were only used for the

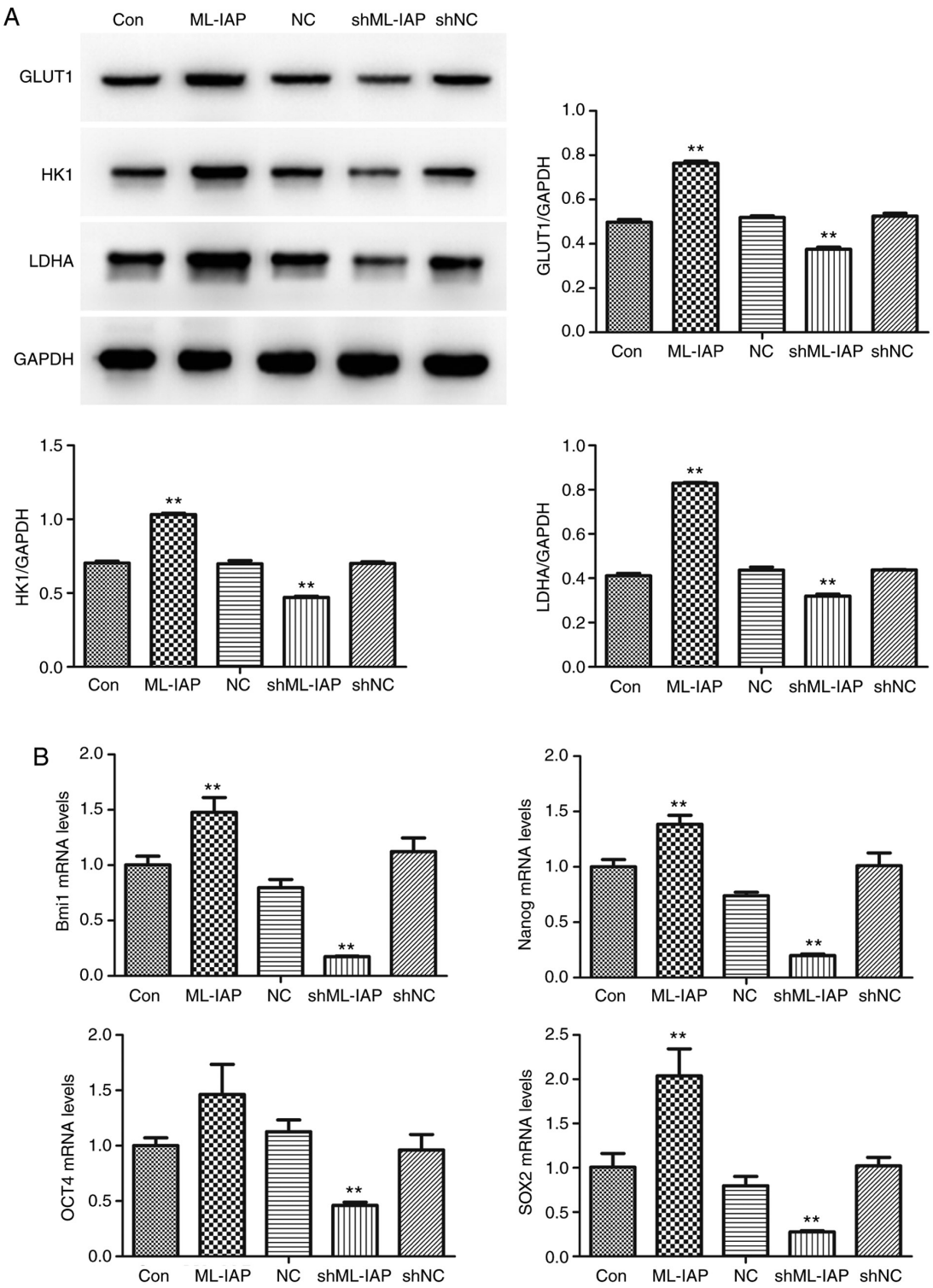

Figure 5. Downregulation of ML-IAP suppresses the metabolism and stemness maintenance of P19 cells. (A) The expression of cell metabolism-related proteins glucose transporter 1, hexokinase 1 and lactate dehydrogenase-A was detected by western blot analysis. (B) The mRNA expression levels of Bmi1, Nanog, octamer-binding transcription factor 4 and sex determining region Y-box 2 in P19 cells were detected by reverse transcription-quantitative PCR. Data are presented as the mean ± SD (n=3). **P<0.01 vs. Con. ML-IAP, melanoma IAP; GLUT1, glucose transporter 1; HK1, hexokinase 1; LDHA, lactate dehydrogenase-A; OCT4, octamer-binding transcription factor 4; SOX2, sex determining region Y-box 2; sh, short hairpin; NC, negative control.

experiments, which is one of the limitations of the present study; therefore, multiple cell lines will be obtained to verify the experimental results in the subsequent experiments.

In conclusion, our findings provided an explanation for the molecular mechanism of ML-IAP silencing in preventing the development of P19 testicular teratoma cells, which occurs by inhibiting cell proliferation and inducing cell cycle arrest and apoptosis. Furthermore, ML-IAP silencing induced caspase activation and suppressed stemness maintenance by inhibiting the Warburg effect in P19 cells. Thus, ML-IAP may be a critical cellular factor, the downregulation of which stimulates apoptosis and contributes to the treatment of testicular teratoma.

Acknowledgements

Not applicable.

Funding

No funding was received.

Availability of data and materials

The datasets used and/or analyzed during the current study are available from the corresponding author on reasonable request.

Authors' contributions

GL and ML designed the experiments. SL, JY, JW and WL performed most of the experiments. CY and HXu drafted the manuscript and analyzed the data. HXi and HC analyzed the data. GL and ML confirmed the authenticity of all the raw data. All the authors have read and approved the final manuscript.

Ethics approval and consent to participate

The present study was approved by the Ethics Review Committee of Wuhan Children's Hospital (Wuhan, China), and the guardians of all patients provided written informed consent to participate in the present study and to provide samples for subsequent experiments.

Patient consent for publication

Not applicable.

Competing interests

The authors declare that they have no competing interests.

References

1. Karmazyn B, Weatherly DL, Lehnert SJ, Cain MP, Fan R, Jennings SG, Ouyang F and Kaefer M: Characteristics of testicular tumors in prepubertal children (age 5-12 years). J Pediatr Urol 14: 259.e1-259.e6, 2018.
2. Juliachs M, Muñoz C, Moutinho CA, Vidal A, Condom E, Esteller M, Graupera M, Casanovas O, Germà JR, Villanueva A and Viñals F: The PDGFRβ-AKT pathway contributes to CDDP-acquired resistance in testicular germ cell tumors. Clin Cancer Res 20: 658-667, 2014.
3. Wang X, Xu S, Tang D, Li M, Wu D and Huang Y: Prepubertal testicular and paratesticular tumors in China: A single-center experience over a 10-year period. J Pediatr Surg 47: 1576-1580, 2012.
4. Berney DM, Lu YJ, Shamash J and Idrees M: Postchemotherapy changes in testicular germ cell tumours: Biology and morphology. Histopathology 70: 26-39, 2017.
5. Rathore R, McCallum JE, Varghese E, Florea AM and Büsselberg D: Overcoming chemotherapy drug resistance by targeting inhibitors of apoptosis proteins (IAPs). Apoptosis 22: 898-919, 2017.
6. Kocab AJ and Duckett CS: Inhibitor of apoptosis proteins as intracellular signaling intermediates. FEBS J 283: 221-231, 2016.
7. Mohamed MS, Bishr MK, Almutairi FM and Ali AG: Inhibitors of apoptosis: Clinical implications in cancer. Apoptosis 22: 1487-1509, 2017.
8. Fulda S: Molecular pathways: Targeting inhibitor of apoptosis proteins in cancer-from molecular mechanism to therapeutic application. Clin Cancer Res 20: 289-295, 2014.
9. Rada M, Nallanthighal S, Cha J, Ryan K, Sage J, Eldred C, Ullo M, Orsulic S and Cheon DJ: Inhibitor of apoptosis proteins (IAPs) mediate collagen type XI alpha 1-driven cisplatin resistance in ovarian cancer. Oncogene 37: 4809-4820, 2018.
10. Checinska A, Hoogeland B, Rodriguez JA, Giaccone G and Kruyt FA: Role of XIAP in inhibiting cisplatin-induced caspase activation in non-small cell lung cancer cells: A small molecule Smac mimic sensitizes for chemotherapy-induced apoptosis by enhancing caspase-3 activation. Exp Cell Res 313: 1215-1224, 2007.
11. Dawood S, Austin L and Cristofanilli M: Cancer stem cells: Implications for cancer therapy. Oncology (Williston Park) 28: 1101-1107, 1110, 2014.
12. Jordan CT, Guzman ML and Noble M: Cancer stem cells. N Engl J Med 355: 1253-1261, 2006.
13. Trosko JE: Evolution of energy metabolism, stem cells and cancer stem cells: How the Warburg and Barker hypothesis might be linked. BMC Proc 7 (Suppl 2): K8, 2013.
14. Pacini N and Borziani F: Cancer stem cell theory and the warburg effect, two sides of the same coin? Int J Mol Sci 15: 8893-8930, 2014.
15. Vaupel P, Schmidberger H and Mayer A: The Warburg effect: Essential part of metabolic reprogramming and central contributor to cancer progression. Int J Radiat Biol 95: 912-919, 2019.
16. Schwartz L, Supuran CT and Alfarouk KO: The warburg effect and the hallmarks of cancer. Anticancer Agents Med Chem 17: 164-170, 2017.
17. Ji J, Yu Y, Li ZL, Chen MY, Deng R, Huang X, Wang GF, Zhang MX, Yang Q, Ravichandran S, *et al*: XIAP limits autophagic degradation of Sox2 and is a therapeutic target in nasopharyngeal carcinoma stem cells. Theranostics 8: 1494-1510, 2018.
18. Ausserlechner MJ and Hagenbuchner J: Mitochondrial survivin-an Achilles' heel in cancer chemoresistance. Mol Cell Oncol 3: e1076589, 2015.
19. Livak KJ and Schmittgen TD: Analysis of relative gene expression data using real-time quantitative PCR and the 2(-Delta Delta C(T)) method. Methods 25: 402-408, 2001.
20. Galli UM, Sauter M, Lecher B, Maurer S, Herbst H, Roemer K and Mueller-Lantzsch N: Human endogenous retrovirus rec interferes with germ cell development in mice and may cause carcinoma in situ, the predecessor lesion of germ cell tumors. Oncogene 24: 3223-3228, 2005.
21. Vucic D, Stennicke HR, Pisabarro MT, Salvesen GS and Dixit VM: ML-IAP, a novel inhibitor of apoptosis that is preferentially expressed in human melanomas. Curr Biol 10: 1359-1366, 2000.
22. Ashhab Y, Alian A, Polliack A, Panet A and Ben Yehuda D: Two splicing variants of a new inhibitor of apoptosis gene with different biological properties and tissue distribution pattern. FEBS Lett 495: 56-60, 2001.
23. Deveraux QL, Roy N, Stennicke HR, Van Arsdale T, Zhou Q, Srinivasula SM, Alnemri ES, Salvesen GS and Reed JC: IAPs block apoptotic events induced by caspase-8 and cytochrome c by direct inhibition of distinct caspases. EMBO J 17: 2215-2223, 1998.
24. Roy N, Deveraux QL, Takahashi R, Salvesen GS and Reed JC: The c-IAP-1 and c-IAP-2 proteins are direct inhibitors of specific caspases. EMBO J 16: 6914-6925, 1997.
25. Green DR and Evan GI: A matter of life and death. Cancer Cell 1: 19-30, 2002.
26. Epstein T, Gatenby RA and Brown JS: The Warburg effect as an adaptation of cancer cells to rapid fluctuations in energy demand. PLoS One 12: e0185085, 2017.
27. Vander Heiden MG, Locasale JW, Swanson KD, Sharfi H, Heffron GJ, Amador-Noguez D, Christofk HR, Wagner G, Rabinowitz JD, Asara JM and Cantley LC: Evidence for an alternative glycolytic pathway in rapidly proliferating cells. Science 329: 1492-1499, 2010.
28. Wang YD, Li SJ and Liao JX: Inhibition of glucose transporter 1 (GLUT1) chemosensitized head and neck cancer cells to cisplatin. Technol Cancer Res Treat 12: 525-535, 2013.
29. Visvader JE and Lindeman GJ: Cancer stem cells in solid tumours: Accumulating evidence and unresolved questions. Nat Rev Cancer 8: 755-768, 2008.
30. Lu Y, Zhu H, Shan H, Lu J, Chang X, Li X, Lu J, Fan X, Zhu S, Wang Y, *et al*: Knockdown of Oct4 and Nanog expression inhibits the stemness of pancreatic cancer cells. Cancer Lett 340: 113-123, 2013.
31. Santini R, Pietrobono S, Pandolfi S, Montagnani V, D'Amico M, Penachioni JY, Vinci MC, Borgognoni L and Stecca B: SOX2 regulates self-renewal and tumorigenicity of human melanoma-initiating cells. Oncogene 33: 4697-4708, 2014.